DEVELOPMENT AND VALIDATION OF ANNULAR FINNED TUBES EVAPORATOR FOR CROSS-FLOW CO-CURRENT EXHAUST GAS - R245FA ORC SYSTEM

Haiam Abbas[1,2], Boaz Habib[1], Mohammed Farid[2]
1, Heavy Engineering Research Association (HERA) / Innovation in Metals
2, The University of Auckland/Chemical and Materials Engineering
haiam.abbas@hera.org.nz

Keywords: *ORC, exhaust gas, R245fa refrigerant, evaporator, annular finned tube, heat exchanger, cross flow gas correlations, HTRI, design optimization, innovation, CFD, ANSYS/CFX.*

ABSTRACT

An in depth analytical study was performed to predict the performance of annular finned tube in staggered array type evaporator used for exhaust gas- refrigerant (R245fa) system in organic Rankine cycle (ORC). The result was compared with simulated performance conducted using the HTRI heat transfer software used for heat exchanger design optimization. CFD studies, using ANSYS/CFX, were also conducted to give an insight on the distribution of the exhaust gas around the fins, the associated pressure drop and the resulting temperature distribution. The performance of the evaporator, in terms of fin efficiency, thermal resistances, dryness (vapour quality), and output temperatures was obtained. Regions that require essential developments were detected and potentials for design innovation were highlighted. At the tube side, improvement is required in regions of single phase flow, while at the exhaust gas side considerable improvements are required. CFD analysis provided information on air flow distribution, pressure, and temperature contours, which can be used for improvement of future designs.

1. BACKGROUND

1.1 Introduction

In organic Rankine cycle (ORC), the technical design of heat exchanger should follow the requirements of the cycle it is designed for. The quality and quantity of heat source available, properties of the working fluid, and the performance and effectiveness of the design in delivering the maximum possible heat loads should all be considered. In the evaporator the liquid stream is heated to a saturation level then gradually evaporated depending on the amount of heat received. Based on heat transfer efficiency and properties of the working fluid, the number of rows required to achieve certain degrees of evaporation/condensation is determined. When air-cooled condenser is used in geothermal plants (Yilmaz et al. 2015), it is essential to account for the cost associated with the fan performance. The specific power consumed by the fan of an air-cooled condenser is 0.15 kW per kg/s of air flow (Toffolo et al. 2014). According to heat exchanger design textbooks, the high cost of air heated/cooled exchangers is related to their large size, which is attributed to high thermal resistance (1/hA) on the gas side due to low heat transfer coefficients (h= 5-20 W/m^2K). One of the main approaches to resolve this issue is to increase the air side heat transfer surface area (A) primarily using extended surfaces (fins).

The focus of this paper has been to improve the existing air/ refrigerant ORC system. Efforts were dedicated toward the design process based on reported correlations suitable for conditions of this study. The results were compared to the ones obtained using the heat transfer research institute (HTRI) and CFD simulations. The HTRI results (temperatures, and vapour quality) were obtained in collaboration with an AGGAT partner. Using Excel, the calculations were carried out on the basis of row by row method using several reported correlations. Accordingly, a design sheet was constructed. Inlets and outlets temperatures of both the exhaust gas and the refrigerant (R245fa) were calculated at each row based on mass and heat balance. The number of rows was specified based on the temperature and vapour quality requirements. Accordingly, several design key points were used as a reference:

1. The lowest cost possible by examining the total number of tube passes required to achieve close temperature and vapour quality approaches.

2. The highest performance possible, drawn based on extensive optimization study.

1.2. Selection of Working Fluid

In recent study, Mastrullo et al. (2015) performed a review about the choice of a suitable organic working fluid and indicated that refrigerants such as R245fa, R236ea, R124, R227ea, R290, can be employed in ORC and indicated that superheat levels are not necessary. This may be of significant importance in geothermal low temperature application.

Fluids with low values of critical temperature, like Novec649, RE347mcc, R245fa, were recommended to optimize the defect of ORC efficiency, whilst fluids with high values of thermal conductivities and latent heats of vaporization were selected in order to minimize the required heat exchanger area. Wang et al. (2011) found out that fluids with low specific heats and high vaporization latent heats are preferable for use in ORC. In another study, Wang et al. (2011) stated that considering safety levels and environmental impacts, R245fa and R245ca are the most suitable working fluids for an engine running on waste heat-recovery system, compared to a list of refrigerant (R11, R141b, R113 and R123), shown in Figure 1. Fiaschi et al. (2014) indicated that n-butane and R245fa are the best performing fluids used for high temperature and heat demands ORC systems. In the same way, Budisulistyo and Krumdieck (2015) highlighted that n-pentane requires the smallest heat transfer area, and hydro-fluorocarbons with low critical temperature such as R245fa and R134a are suitable for binary ORC. It can be concluded that R245fa and n-pentane are the best working fluids selected for high geothermal temperature loads.

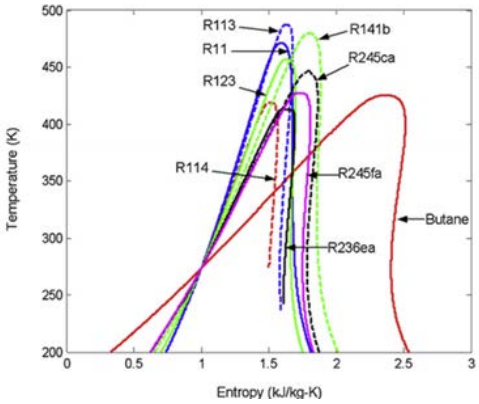

Figure 1: Schematic of *Temperature-Entropy diagram* of selected working fluids (Wang et al. 2011).

1.2 Advanced Heat Exchanger for Enhanced Performance

Considering utilization of refrigerant fluids as analysed above for heat transfer, a variety of approaches have been explored to enhance heat transfer including internally and externally finned tubes, as illustrated in Figure 2. The most highly recommended fins are slit and serrated type. Slit fins were studied by Byuna et al. (2007), who reported that heat transfer rate with slit fins provided an improvement of the order of 54% compared to that of plate fins. At cases where air velocity was in the range of 2.4 m/s and the refrigerant was R-22, the wavy fins showed extra 4.6% improvement compared to that with plate fins. Serrated fins were also examined, in another study (Peng et al. 2012), where the cooling performance of serrated fins performed better than plain fins using the same structural parameters. However, the enhancement achieved by using serrated fins or triangle fins was reduced at Reynolds number levels, as reported by Li et al. (2013). Similarly, the enhancement in performance of herringbone micro-fin tubes diminishes above such levels.

Likewise, Wang et al. (2015) carried out a comparative study between plain, louver, and semi-dimple vortex generator fins on the airside performance of fin-and-tube heat exchangers. Different fin pitch were tested, being 1.6 mm and 2.0 mm using different numbers of tube rows (1-4). The results showed a high dependency on the resulting swirled motion of the semi dimple vortex. The effect of the number of tube rows on the heat transfer coefficients was negligible.

To predict the performance of fins with new configuration in plate-fin heat exchangers and to investigate the pressure drop and heat transfer characteristics over serrated fins at low Reynolds number, numerical modelling methods were performed by Peng and Ling (2008). Recent study on helical-coiled, crimped, spiral, finned-copper tube heat exchanger in dry surface conditions was presented (Boonsri and Wongwises 2015) based on theoretical and experimental data. The authors reported that modelling turbulence in complex geometries, such as those of finned tubes, is difficult without the aid of CFD techniques.

An alternative to finned tube is porous media (Hooman 2015). A number of correlations were proposed to predict the total pressure drop and heat transfer of extended surfaces.

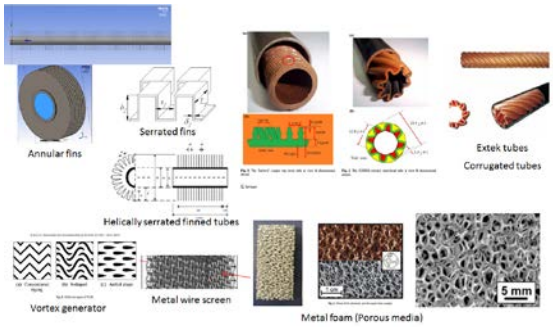

Figure 2: Examples of different approaches for the enhancements of heat transfer.

Innovative design projected by Vahab et al. (2005) was applied on the plate side of the plate heat exchanger using offset strip fins along the path of the air to control the direction of the air and drive the flow to regions of stagnant velocity at vicinities behind the tubes. The pressure drop was reduced and the thermal boundary layer was periodically disturbed at each fin strip leading to 80% increase in heat transfer coefficient. Accordingly, lower pressure drops, less surface area and smaller ground coverage could be obtained compared to fin-and-tube type heat exchanger.

Imran et al. (2015) presented an optimization study based on Genetic Algorithms results performed on chevron type plate (1.25 mm length x 0.55 mm width) evaporator. The objective was to have a compromise between pressure drop and cost of evaporator. The optimization study indicated that the plate length has significant effect on pressure drop and cost of evaporator. The optimum value of allowable pressure drop of 30–40 kPa was used, corresponding to a net power of 73–74 kW of ORC system and cost of evaporator of 3000–3500$.

In all these CFD studies, the main improvement in heat transfer was achieved as a result of the enhanced distribution of air flow and the increase in the area associated with the heat transfer. A typical annular finned tube heat exchanger was selected as a reference-point design. The influence of different annular fin sizes and distances on air flow and heat transfer was examined using CFD and known heat transfer correlations as explained in section 1.3.1. Essentially, the design sheet was employed to quantify the vales of the thermal resistances in the direction of heat transfer to aid the design process

1.3 An Overview of Heat Exchanger Design Process

The design process of heat exchanger is normally referred to as being an art as much as a science, as reported in the main engineering handbook (Perry and Green). In many heat exchanger design books, researchers are more often interacted with a challenging statement indicating that the calculations carried out to design heat exchangers are far from exact. This indicates that the design of heat exchangers is a challenging process. Literature was reviewed, mostly based on heat transfer text books (Bergman et al. 2011, John H. Lienhard (2011), Holman 2010, and Mills 1992) and examining new techniques and innovations in heat exchanger design reported in papers. It was realized that there are considerable discrepancies (10-100% or sometimes up to 200%) between experimental results and those obtained using very-well known two-phase empirical correlations. The variations in operating fluids and working conditions are the main reason behind such discrepancies.

Therefore, experimental validation is a requirement for any constructed model to increase confidence.

For more reliable design process, there has been increasing interest in the application of heat transfer software to carry out the actual calculations and to predict the performance of heat exchanger. One of the more commonly used software for heat exchanger design is from Heat Transfer Research Inc. (HTRI). However they are limited in their ability to give guidance to the best exchanger type and fluid orientations. Computational Fluid Dynamics (CFD) can be used here to understand air distribution which is a major design factor. Using ANSYS-CFX on a high performance computing of NESI, Pan Cluster, of University of Auckland, it was possible to speed up computational work. Profiles of air distribution around the fins were determined. Drawbacks in the design, where regions of low air flow and thus low heat transfer, were designed. Concepts for design improvement and innovation were drawn.

1.3.1 The NTU Method.

The transfer of heat flow (Q), from the hot gas, flowing in cross-flow on a bundle of annular finned tubes in staggered arrangement, illustrated in Figure 3, is calculated (Equations 1-7). Based on row by row method, the effectiveness (ε) and the number of transfer units (NTU) for co-current flow correlations (Equations 2-4) were calculated. At temperatures below and above the saturation levels, equations 3, and 4, were employed, respectively.

$$Q = m^{\cdot} c_{\min} \varepsilon . (T_{h,in} - T_{c,in}) \qquad \text{Equation 1}$$

$$NTU = \frac{UA}{C_{\min}} \qquad \text{Equation 2}$$

$$\varepsilon = \frac{1 - Exp(-(1 + C_{\min}/C_{\max})NTU)}{1 + C_{\min}/C_{\max}} \qquad \text{Equation 3}$$

$$\varepsilon = 1 - Exp(-NTU) \qquad \text{Equation 4}$$

The overall heat transfer coefficient (U) is derived (Equation 5), from the thermal resistances between the hot gas (shell side) and the working fluid (tube side):

$$\frac{1}{UA} = \frac{1}{A_0 h_o \eta_o} + \frac{\ln(r_o/r)_i}{2\pi L k} + \frac{1}{A_i h_i} \qquad \text{Equation 5}$$

Where A, h, η_f, r, L, k, are the area, convective heat transfer coefficient, fin overall efficiency (Equation 6), tube radius, tube length, and thermal conductivity of the tube, respectively. The subscripts, *o*, *i*, and *f*, stands for the outside, inside, and fin, correspondingly. The overall fin surface efficiency (η_o) is derived from Equation 6, based on fin efficiency (η_f) of one circular fin, calculated from the modified Bessel functions (Equation 7):

$$\eta_o = 1 - \frac{A_f}{A_o}(1 - \eta_f) \qquad \text{Equation 6}$$

$$\eta_f = \frac{2r_1/m}{(r_{2c}^2 - r_1^2)} * \frac{K_1(mr_1)I_1(mr_2) - I_1(mr_1)K_1(mr_2)}{K_0(mr_1)I_1(mr_2) + I_0(mr_1)K_1(mr_2)} \qquad \text{Equation 7}$$

Where $m = (2h/k)^{1/2}$, $A_f = 2\pi(r_{2c}^2 - r_1^2)$, $r_{2c} = r_2 + t/2$, and A_f, *and* A_o, are the surface area of the fins, and the total surface area of the fins and the bare area of the tube (unfinned), respectively. I_1, and K_1, are modified Bessel functions for the first and second kinds, respectively, and *h*, *k*, and *t* are the convective heat transfer coefficient, thermal conductivity of the fins/tubes, and fin thickness, in the same order.

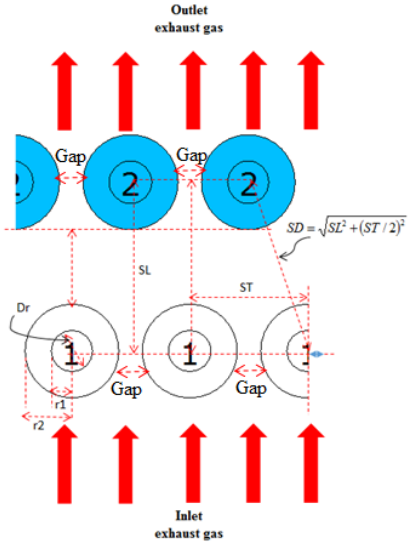

Figure 3: Tube arrangement of the reference design of the heat exchanger.

1.3.2 Heat Transfer Coefficient at the Gas Side

Highly finned tube correlation (Equation 8) on a bundle of tubes was used for conditions where the distance between fins in the range of $0.13 \le s_{fin}/l_{fin} \le 0.57$, and the ratio of transverse to the longitudinal distances in the range of $1.15 \le ST/SL \le 1.72$:

$$Nu = 0.242\,\mathrm{Re}^{0.658}\left(\frac{s_{fin}}{l_{fin}}\right)^{0.297}\left(\frac{ST}{SL}\right)^{-0.091}\mathrm{Pr}^{(1/3)}.F_1.F_2 \qquad \text{Equation 8}$$

Where F1 is correction factor for fluid property between the average bulk temperature and the wall, F2 is correction factor for the number of rows used, and equals unity for rows more than ten.

1.3.3 Heat Transfer Coefficient at the Refrigerant Side

The internal heat transfer coefficient at the refrigerant side is calculated based on the nature of the flow. For single face flow, the Dittus-Boelter equation (9) was employed:

$$h_{lo} = 0023(GD_i/\mu_l)^{0.8}\,\mathrm{Pr}_l^{0.4}\frac{k_l}{D_i} \qquad \text{Equation 9}$$

Whereas $G = m^{\cdot}/A_{in}$ is the mass flux of the total flow at the internal cross-sectional area (A_{in}) of the tube.

For two-phase flow, two phase multiplier approach was followed in literature to calculate the two phase condensation/ vaporization forced convection heat transfer coefficient for several refrigerants, as extensively reviewed

by Awad (2012). The model of interest was Dobson and Chato annular flow correlation (equation 10) suited for flow in both horizontal and vertical tubes. This correlation is based on the convective number (*Co*) (equation 11) and the Lockhart-Martinelli parameter (X_{tt}) for turbulent–turbulent flow (of both the liquid and the vapour), defined in equation 12. At values of Co > 1 (at low quality), nucleate boiling dominates, and two phase heat transfer coefficient increases with increasing the boiling number (Bo) (Equation 13), and becomes independent of Co. As Co decreases (with increasing quality), the effect of Bo declines and heat transfer increases with decreasing Co. Another important parameter, based on the liquid phase only, termed Froude number (Fr), expressed in Equation 13, which is a measure of inertial forces and gravitational forces. Fr number is used to detect regions of flow separation between the vapour and the liquid streams. It was given that Fr < 0.04 indicates that the top of the tube is relatively dry and heat transfer begins to decline, in contrast to that at higher values.

Vapour quality (x) was determined based on the rate of vaporisation/condensation (Q/h_v) determined at each row, from the heat transfer of Equation 1, and latent heat of vaporization/condensation (h_v). The outlet temperature of each stream was calculated based on the sensible heat transfer (Equation 15) at each row. In these equations, properties were calculated at the film temperature. Heats of vaporization/condensation were determined based on the operating pressure. Pressure drops in the evaporator/condenser at the shell and the tube sides were also determined, using the simulations (HTRI and ANSYS-CFX), and validated against theoretical correlations, extensively reviewed in heat transfer textbooks.

$$h = 0.023\left(\frac{k_l}{D_i}\right)\left(G(1-x)D_i/\mu_l\right)^{0.8}\mathrm{Pr}_l^{0.4}\left(1+\frac{2.22}{X_{tt}^{0.89}}\right) \quad \text{Equation 10}$$

$$Co = \left(\frac{1-x}{x}\right)^{0.9}\left(\frac{\rho_v}{\rho_l}\right)^{0.5} \quad \text{Equation 11}$$

$$X_{tt} = Co\left(\frac{\mu_l}{\mu_v}\right)^{0.125} \quad \text{Equation 12}$$

$$Bo = \frac{Q/L}{Gh_v} \quad \text{Equation 13}$$

$$Fr = \frac{G^2}{\rho_l^2 g d_i} \quad \text{Equation 14}$$

1.3.4 CFD Model

The optimization process regarding fin size and its associated influence on the distribution of the exhaust gas was performed using the CFD modelling package ANSYS/CFX. Different CFD models were developed such as shown in Figure 3. Additional three models of different fin numbers (highly finned, 40%, and 60% less fins, were also generated for design optimization study. Models of different spacing, in terms of ST, SL, and fins length were also prepared. The models were discretised using smart meshing method, where high mesh density is applied at regions where large gradient is expected. This was applied at surfaces associated with the heat transfer (fins surfaces and working fluid internal tube walls). However, coarse mesh was avoided in all cases. Unstructured mesh was applied of mesh statistics depending on the size of the model; for five fins slice model 221334 node, and 842600 elements were required forming 15 MB of model size.

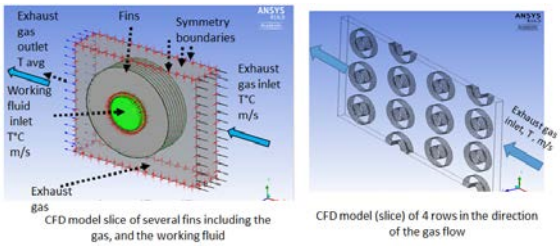

Figure 4: CFD models details.

Steady state simulation type was solved using the default basic control settings of CFX solver, of High Resolution option for both advection scheme and turbulence numeric.

Turbulent flow (Reynold number, gas >2000, working fluid > 25000) was modelled using the widely tested, advanced model for boundary layer flows under adverse pressure gradient, the Shear Stress Transport (SST), of Menter (Menter 1992, Menter 1993, Menter 1994, Menter and Esch 2001, Menter et al. 2003). This model is based on a series of partial differential equations derived from the well-known Reynolds Averaged Navier-Stokes (RANS) equations. The flow is solved based on blending the basic free stream model $(k-\varepsilon)$ with the boundary layer model $(k-\omega)$, using blending factors ranging from zero (near the wall) to one (outside the wall boundary layer). Detailed descriptions of these equations are found in the CFX theory guide (ANSYS 2009).

2. Results

2.1 Correlations Results

Considering the reference design, the parameters affecting thermal resistances, such as fin efficiency, area, heat transfer coefficients were calculated. Single phase (SP) and two-phase (TP) flow were determined. Fin efficiency was calculated at each row as well as heat transfer coefficient at the gas-side was determined (in the range of 19-22 W/m^{2}K). Two phase heat transfer coefficient (TP HTC) was calculated from several known empirical correlations suited for forced convection condensation and boiling in horizontal and vertical tubes, listed in Figure 5. Most of the listed correlations showed similar trends apparent from two correlations. This is because these correlations are derived for nucleate boiling/condensation. This gave the indication that nucleation is not dominant at high vapour quality levels. In contrast, at low quality levels Co number was in the range (more than one) where nucleate boiling dominates (see section 1.3.3). Apparently, SP HTC is lower than that at TP. Accordingly, regions of SP heat flow requires additional surface enhancements to improve heat transfer. Also, TP HTC at the working fluid increased with an increase in vapour quality. Furthermore, the calculated (Equation 14) values of Fr number were in the favorable range (above 0.04, (Fr > 1)), where dry walls are avoided.

As indicated previously, the selection of TP HTC was based on a comparison with results of vapour fraction (quality) and temperatures obtained using the HTRI simulation. Dobson and Chato correlation was selected based on the closest agreement with the HTRI results. Using the selected correlations, sensitivity analysis was conducted to investigate the effect of fin parameters on the overall

performance of the evaporator. Most importantly, regions of large thermal resistances in the direction of the heat transfer were identified, as shown in Figure 6. However, since experimental results are still required to support the validation process, an underway plan was started for the construction of the required experimental test rig. This will be covered in further studies.

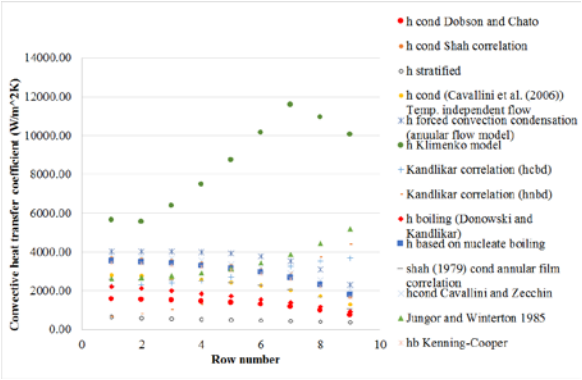

Figure 5: Correlations results for convective heat transfer for two phase flow at the refrigerant region.

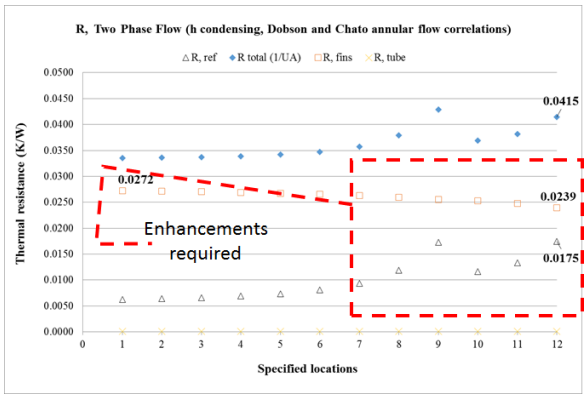

Figure 6: Thermal resistances in the direction of heat transfer calculated based on the correlation results obtained using Excel.

2.2 Fin Optimization Study

Two fin heights (the basecase and 22.4% larger), and four different thermal conductivities of the fins and the tubes, along with different scenarios in terms of ST and SL were studied. The correlation results, based on Excel, were also employed to predict the performance of the fins. It was found that fin efficiency is highly influenced by fin thermal conductivity and fins length (height). Low dependency was found on SL, while larger dependency was pronounced on ST. Likewise, detailed performance of the fins were examined to get insight on the associated interactions between the exhaust gas and the fins. The performance of the fins was examined based on the resulting increase in temperature calculated at the outlet boundary of the working fluid. Thermal conductivity impact of different materials was also evaluated for cases counted as those of tight conditions (ST values just above the diameter of the fins leading to a decrease in the openings between the transverse rows).

Temperature contours of fins with different thermal conductivities, at normal transverse spacing (loose), are shown in Figure 7. Homogenius temperature distributions at the fins were found for cases with copper and aluminium fins, in contrast to that of the rest, where inefficient temperature distribution was observed. The reason for that was the low conductivity of fins. It was found that the resulting temperature with copper and aluminium fins were comparable, while considerably lower (7% and 18%) for carbon steel and steel fins, respectively, as can be seen in Figure 8. No noticable impact was found on the associated distribution of the gas flow or pressure drop.

Larger models will show considerable increase in temperatures at the working fluid side. This is due to the increase in the surface area of heat transfer, compared to this study. However, the slice models gave reliable indications about the level of influence and thereby can be successfully employed in sensitivity studies.

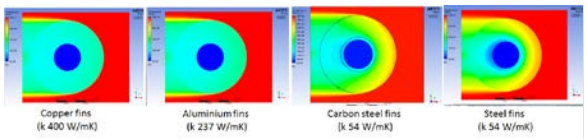

Figure 7 : CFD temperature results with different thermal conductivities, at plane passing in the middle of the fins.

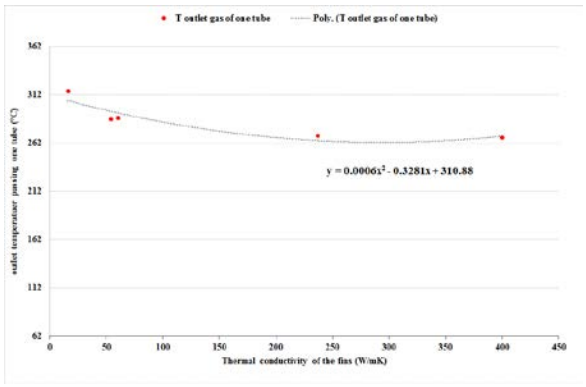

Figure 8 : Average temperature of the exhaust gas passing one annular finned tube for different thermal conductivities.

The optimum fin length was also calculated, based on infinite fin approach. As can be noted in Figure 9, there is a potential to operate with fin height (starting from the surface of the bare tube) of up to 0.12 m. After this no significant heat transfer improvement can be obtained as a result of reaching equilibrium levels with the surroundings (exhaust gas). Nevertheless, a compromise had to be made to meet obligations in terms of size requirements of the heat exchanger and market availability of the required fin size.

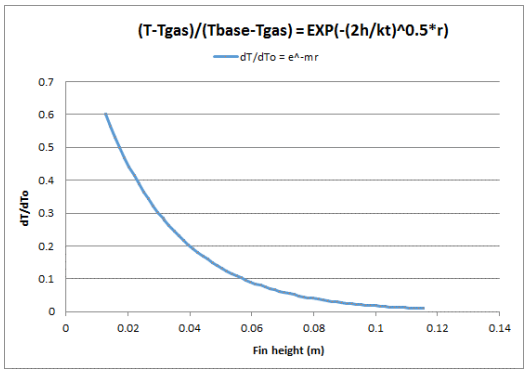

Figure 9 : Potential range for effective fin height calculated based on the assumption of infinite fin length.

Taking into consideration size limitation and cost, the assessment was based on providing the maximum possible temperature increase at the working fluid side. Two cases were compared with the reference design. One with 22.4% larger fins, where the flow area between the tubes experienced considerable reduction as a results of fin size increase. The result of this case is shown in Figure 10.

The larger fins case resulted with enhanced temperature distribution as a result of effective capture to the high temperature streams (red zones) directly at the first row, in contrast to the basecase design, where two rows were required to achieve similar performance. Also, regions of low temperatures were formed clearly behind each tube at the reference design, while those have been eliminated with the case of larger fins and small gaps. This was examined further in the second case, where fin height was kept the same (as the reference design) while ST was decreased considerably to provide equivalent gaps between the tubes, in the transverse orientation, compared to that obtained with 22.4% larger fins.

It was apparent that applying such tightness provided significant enhancement to the temperature increase at the working fluid side for the two cases compared to the poor performance of the reference case, as shown in Figure 11. This draws the conclusion that in situations where fin enlargements pose complicated technical problems, the simple and practical approach is to decrease the gaps between the transvers tubes to the minimal. This impact was re-examined for cases with three different thermal conductivities. No noticeable difference was found, on the exhaust gas distribution, between the three cases, as shown in Figure 12. Consistency in the performance was maintained for fins with copper and aluminum, where the highest temperature increase was found at the working fluid side compared to that with lower thermal conductivity fins. In terms of pressure, the associated pressure drop was doubled compared to that of the reference case (loose gaps), but the increase was still with the acceptable range (up to 10 Pa per a model equivalent to about 150 Pa per the whole heat exchanger at the exhaust gas side.

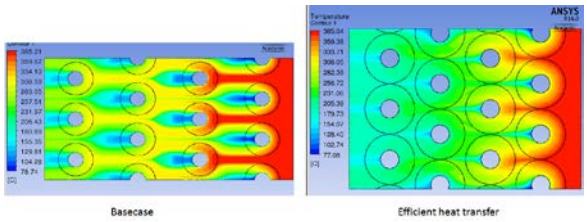

Figure 10 : Temperature contours of the basecase and that of 22.4% larger fins, showing streams of high temperatures are effectively captured at the first row of the model with larger fins.

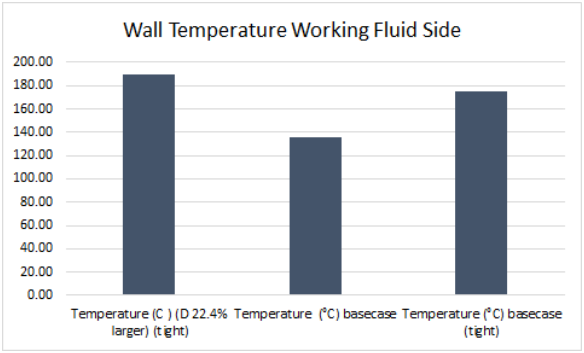

Figure 11 : Wall temperature at the working fluid side for three different cases obtained from the CFD slice model.

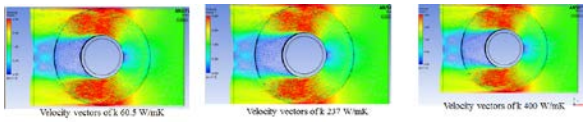

Figure 12 : Velocity vectors at tight geometry conditions for three different thermal conductivities.

In relation to fins number, the influence of fins number on the resulting temperature of the fins is shown in Figure 13, for cases with loose gaps. The associated impact on the distribution of the exhaust gas is shown in Figure 14. Apparently, with lower number of fins, regions of low velocity increased and streams of high temperatures freely escaped fin surfaces where effective heat transfer is taking place. This was examined from the resulting temperature increase at the outlet boundary of the working fluid. Larger temperature increase was realized in the case of highly finned tube (reference case).

To draw a conclusion, more studies are required especially in cases with tight conditions where considerable improvement in the heat transfer was observed. Major improvements are required in relation to the position of the inlet of the exhaust gas. Multiple inlets might resolve the issue of low velocity regions formed as a result of the shedding effect of the tubes. The application of different techniques, such as porous media, instead of the annular fins will have direct impact on the distribution of the exhaust gas and will ensure the maximum interaction between the gas and the associated areas with heat transfer. These might be covered in future work.

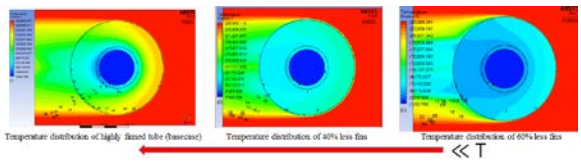

Figure 13: Temperature contours at plane passing in the center of the fins and the working fluid from the inlet to the outlet of the exhaust gas for three different fins number.

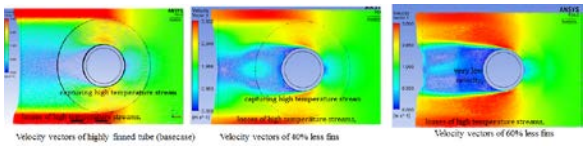

Figure 14 : Velocity vector for three cases (with loose gaps) of different fins number.

3. Conclusions

Several important findings were drawn from this work using existing correlation and the HTRI and ANSYS-CFX CFD analysis, as follow:

- Dobson and Chato annular flow correlation suited for flow in both horizontal and vertical tubes resulted in closest agreements with the HTRI simulation results, in terms of vapour quality and temperatures. However, experimental results are required for the validation process, before the implementation for expert design tool objective.

- CFD studies provided insight on the interactions between the air flow and the existing surfaces associated with the heat transfer. Different design parameters will be examined in further studies.

- Regions of high thermal resistance in the direction of heat transfer are those located mainly at the single-phase flow. This is where considerable enhancement to the heat transfer are required for design developments and innovation.

- Fins made of materials of high thermal conductivity (above 200 W/mK) such as aluminium and copper resulted to maximum enhancement in heat transfer compared to low thermal conductivity (60 W/mK). Transvers distances between adjacent tubes have significant impact on the performance of the heat exchanger

ACKNOWLEDGEMENTS

Vital support was provided by the high performance HPC NESI PAN cluster of the University of Auckland.

REFERENCES

ANSYS, I. (2009). "ANSYS CFX-Solver Theory Guide." http://orange.engr.ucdavis.edu/Documentation12.1/121/CFX/xthry.pdf.

Awad, M. M. (2012). "Two-Phase Flow." from http://creativecommons.org/licenses/by/3.0.

Boonsri, R. and S. Wongwises (2015). "Mathematical Model for Predicting the Heat Transfer Characteristics of a Helical-Coiled, Crimped, Spiral, Finned-Tube Heat Exchanger." Heat Transfer Engineering 36(18): 1495-1503.

Budisulistyo, D. and S. Krumdieck (2015). "Thermodynamic and economic analysis for the pre-feasibility study of a binary geothermal power plant." Energy Conversion and Management 103: 639-649.

Byuna, J.-S., J. Leeb and J.-Y. Choic (2007). "Numerical analysis of evaporation performance in a finned-tube heat exchanger." International Journal of Refrigeration 30 812-820.

Fiaschi, D., A. Lifshitz, G. Manfrida and D. Tempesti (2014). "An innovative ORC power plant layout for heat and power generation from medium- to low-temperature geothermal resources." Energy Conversion and Management 88: 883-893.

Gungor, K. E. and R. H. S. Winterton (1986). "A general correlation for flow boiling in tubes and annuli." Hear Mass Transfer. 29(3): 351-358.

Hooman, K. (2015). Advanced Air-Cooled Heat Exchangers for Geothermal Power Plants. Proceedings World Geothermal Congress. Melbourne, Australia.

Imran, M., M. Usman, B.-S. Park, H.-J. Kim and D.-H. Lee (2015). "Multi-objective optimization of evaporator of organic Rankine cycle (ORC) for low temperature geothermal heat source." Applied Thermal Engineering 80: 1-9.

John H. Lienhard (2011). A Heat Transfer Textbook. Cambridge, Massachusetts, U.S.A.

Jung, D., K.-h. Song, Y. Cho and S.-j. Kim (2003). "Flow condensation heat transfer coefficients of pure refrigerants." International Journal of Refrigeration 26: 4-11.

Li, J., X. Ling and H. Peng (2013). "Field synergy analysis on convective heat transfer and fluid flow of a novel triangular perforated fin." International Journal of Heat and Mass Transfer 64: 526-535.

Mastrullo, R., A. W. Mauro, R. Revellin and L. Viscito (2015). "Modeling and optimization of a shell and louvered fin mini-tubes heat exchanger in an ORC powered by an internal combustion engine." Energy Conversion and Management 101: 697-712.

Menter, F. and T. Esch (2001). Elements of industrial heat transfer predictions

Proceedings of COBEM 2001, invited lectures, 16th Brazilian congress of mechanical engineering (XVI Congresso Brasileiro de Engenharia Mecânica), . Uberlândia, Brazil, vol 20, pp 117-127.

Menter, F. R. (1992). Improved Two-Equation k-ω Turbulence Models for Aerodynamic Flows. NASA Technical Memorandum 103975, Ames Research Center.

Menter, F. R. (1993). Zonal two equation k-ω turbulence models for aerodynamic flows. 24th fluid dynamics conference, no. AIAA-93-2906, AIAA, . Orlando, Florida, USA: pp. 1-21.

Menter, F. R. (1994). "Two-equation eddy-viscosity turbulence models for engineering applications" AIAAJ, 32 , pp 1598-1605.

Menter, F. R., M. Kuntz and R. Langtry (2003). Ten years of industrial experience with the SST turbulence model. Turbulence, heat and mass transfer 4: proceedings of the fourth international symposium on turbulence, heat and mass transfer, turbulence heat and mass transfer series.Peng, H. and X. Ling (2008). "Numerical modeling and experimental verification of flow and heat transfer over serrated fins at low Reynolds number." Experimental Thermal and Fluid Science(32): 1039-1048.

Peng, H., X. Ling and J. Li (2012). "Numerical simulation and experimental verification on thermal performance of a novel fin-plate thermosyphon." Applied Thermal Engineering 40: 181-188.

Perry, R. H. and D. W. Green "Perry's Chemical Engineeerings' Handbook." Seven Edition.

Shah, M. M. (1979). "A General correlation for Heat Transfer During film condensation Inside Pipes" Heat Mass Transfer 22: 547-556.

Toffolo, A., A. Lazzaretto, G. Manente and M. Pac (2014). "A multi-criteria approach for the optimal selection of working fluid and design parameters in Organic Rankine Cycle systems." Applied Energy 121(219-232).

Vahab, H., D. James and B. K. J (2005). "The Fin-on-Plate Heat Exchanger: A New Configuration for Air-Cooled Power Plants." Heat Transfer Engineering 26(6): 7-15.
Wang, C.-C., K.-Y. Chen, J.-S. Liaw and C.-Y. Tseng (2015). "An experimental study of the air-side performance of fin-and-tube heat exchangers having plain, louver, and semi-dimple vortex generator configuration." International Journal of Heat and Mass Transfer 80: 281-287.
Wang, E. H., H. G. Zhang, B. Y. Fan, M. G. Ouyang, Y. Zhao and Q. H. Mu (2011). "Study of working fluid selection of organic Rankine cycle (ORC) for engine waste heat recovery." Energy 36(5): 3406-3418.
Yilmaz, C., M. Kanoglu and A. Abusoglu (2015). "Thermoeconomic cost evaluation of hydrogen production driven by binary geothermal power plant." Geothermics 57: 18-25.